

Dynamic Behavior of Natural Rubber During Large Extensions

J. A. C. HARWOOD and A. SCHALLAMACH,
*The Natural Rubber Producers' Research Association,
Welwyn Garden City, Herts., England*

Synopsis

The stresses and energy losses during simple extension cycles up to a maximum elongation of 530% have been determined for an unfilled vulcanizate of natural rubber as a function of the temperature and extension rate. At sufficiently short elongation times and low temperatures, the rate and temperature dependence of the ascending stresses are connected by the Ferry transform, and the superposition principle can be applied to them. Outside this experimental range, the stresses are increased by crystallization. The validity of the Ferry transform for the energy losses and the energy loss ratio is more restricted than for the stresses, and the losses are always higher than can be expected from a purely viscoelastic mechanism. The additional losses are tentatively ascribed to incipient crystallization and stress-softening effects. At short elongation times and low temperatures, the losses approach the values predicted by viscoelasticity, and the loss ratio becomes independent of the maximum extension of the strain cycle.

INTRODUCTION

The literature dealing with the dynamic properties of rubber at moderate and large strains, though sparse, has elicited the following experimental facts. The temperature and rate dependence of the stress at a given extension are interrelated by means of the Ferry transform;¹ the family of curves giving the stress at various temperatures as a function of the logarithm of the rate are superimposable by temperature-dependent horizontal shifts to produce a master curve at the chosen reference temperature. The magnitude of the shifts is ruled by the same universal law which connects rate and temperature dependence of viscoelastic properties generally.

This result has been established for polyisobutylene,² styrene-butadiene rubber (SBR),^{3,4} and acrylonitrile-butadiene rubber (ABR).⁵ The exception is natural rubber (NR) at higher strains in the range of rates and temperatures where crystallization is expected to interfere with the purely viscoelastic mechanisms.⁵

All the previous studies have also indicated that the stress can be factorized as the product of two functions: one function depends only on the strain, and the other only on the time taken to reach this strain. This finding has led to a great simplification in the presentation of the results

because the strain and time functions can be interpreted in physically meaningful terms.

At low temperatures and for high rates of elongation the stress-strain curves develop a maximum at low strains, and simple factorization of the stress is no longer possible, but the sum of two products, each with different stress and time functions, gives a fair description of the data.⁵

Previous work on NR at moderate strains has now been expanded to large strains, with special reference to the energy losses incurred in a strain cycle.

EXPERIMENTAL

The tensometer used in the investigation has been described in an earlier publication,⁵ but the specimen holders were modified. The ring samples (1.8 cm. diameter), instead of being elongated between pins, were stretched between two couples of small roller bearings, as employed by Grosch and Schallamach,⁶ in order to ensure uniform extension.

Temperature control above room temperature was achieved by immersing the samples in thermostatically controlled water and below room temperature, by immersion in alcohol circulated through a Minus Seventy thermostat. The rubber was an unfilled, conventional vulcanizate of NR.* The samples were cut out of sheets with a rotating two-bladed tool.

PROCEDURE

Application of a stress to a new rubber sample reduces its initial stiffness. This effect, which occurs both in gum and filled rubbers, has been studied in detail by Mullins and Tobin⁷ and Harwood et al.,^{8,9} reproducible curves are obtained after several stretches. For this reason, the samples were subjected before the experiment to eight extension cycles with a maximum elongation of 600% at room temperature. After resting for 5 min. the samples retained a small permanent set, and strains were referred to this "conditioned" length as calculated from their mean diameter and weight. The procedure was repeated when the sample had been resting for a prolonged time. Each sample was used for several measurements and periodically checked at a standard temperature and rate of elongation for signs of deterioration. After measurements below room temperature the samples were removed from the bath to expedite relaxation and allow crystallization effects to disappear.

Stress-strain cycles were recorded for three different maximum strains at the temperatures and strain rates listed in Table I.

* Composition of the samples (by weight): smoked sheet RSS1, 100 parts; zinc oxide, 5 phr; stearic acid, 3 phr; Dutrex R, 2 phr; Santocure, 0.7 phr; sulfur, 2.5 phr; Nonox HFN, 1 phr. Cure: 40 min. at 140°C.

TABLE I

Maximum strain in cycle, %	Temperature, °C.	Strain rate, %/sec.
280	25; 0; -26; -45; -50	0.07-700 in 4 steps
440	25; 13; 0; -13; -26; -35.5; -45	0.07-700 in 8 steps
530	25; 0; -26; -45	0.07-700 in 4 steps

RESULTS

Examples of the stress-strain loops are shown in Figure 1, the ordinate being the stress F on the unstressed cross-sectional area of the conditioned

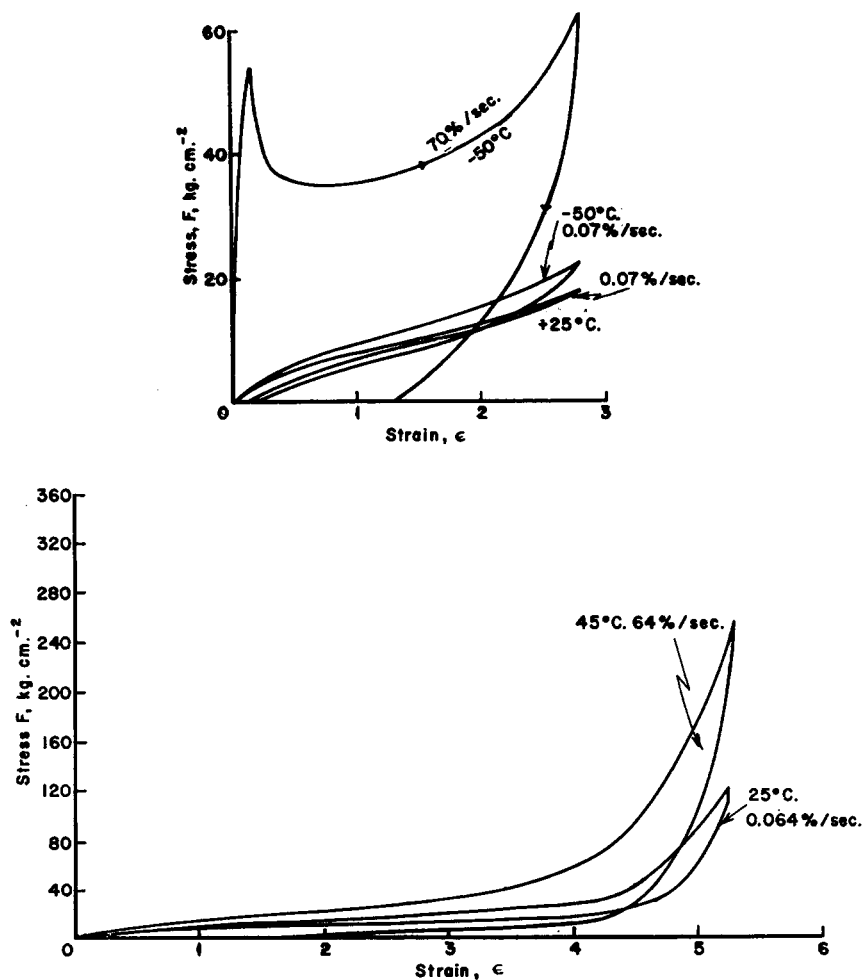


Fig. 1. Examples of stress-strain cycles.

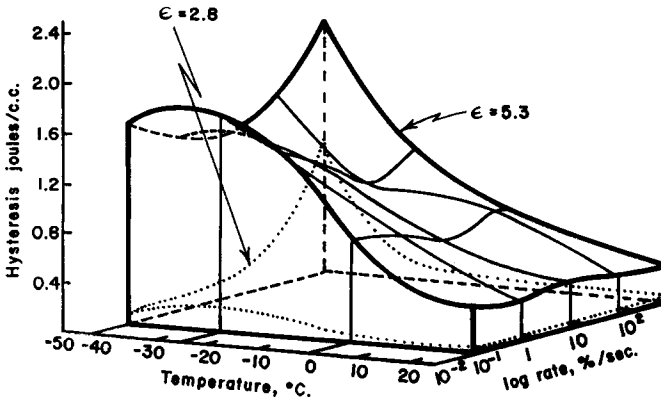


Fig. 2. Energy loss in cycle vs. temperature and strain rate; two maximum extensions, $\epsilon = 2.8$ and 5.3.

specimen. One of the extension curves exhibits a pronounced maximum of the type referred to in the Introduction, followed by a negative characteristic. Mathematical argument based on energy considerations has been invoked to show how this phenomenon can occur without necking or cold drawing taking place.⁵ For corroboratory evidence electronic flash photographs of a straight (as opposed to ring) sample of ABR were taken under conditions of rate and temperature under which a maximum in the extension curve of this material occurs, and again no necking could be observed.

The work of extension and the energy lost during the cycle were determined by graphical integration, and the ratio μ of energy lost to work done was calculated.

The effect of temperature and rate of elongation on the energy losses and the loss ratio μ is illustrated by the three-dimensional plots in Figures 2 and 3 for stress-strain cycles with two different maximum elongations.

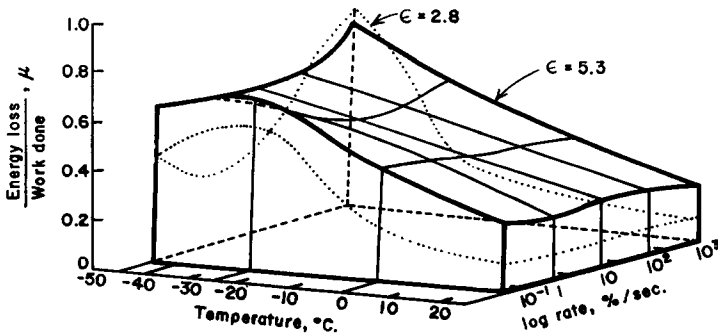


Fig. 3. Energy loss ratio vs. temperature and strain rate; two maximum extensions, $\epsilon = 2.8$ and 5.3.

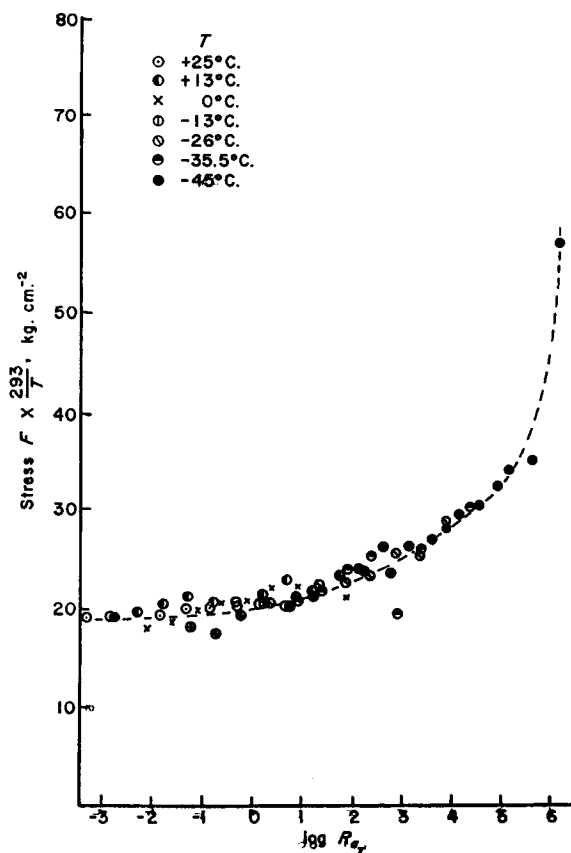


Fig. 4. Master curve of stress vs. strain rate for 300% strain.

DISCUSSION

Strain-Increasing Curves

The construction of master curves for the stress at a given strain as a function of the rate of extension, by horizontal shifts of the curves obtained at different temperature, was only partially successful. This failure of the Ferry transform fully to describe the interrelation between temperature and rate dependence of the stresses was expected from the results obtained at moderate strains.⁵ In order to demonstrate the deviations of the stresses from the values expected from a purely viscoelastic mechanism, a transform was carried out by using the Williams, Landel, and Ferry¹⁰ (WLF) equation for the temperature dependence of the shift factor a_T :

$$\log a_T = -8.86(T - T_s) / [101.6 + (T - T_s)] \quad (1)$$

The standard reference temperature T_s in eq. (1) was taken as -21°C ., as determined by torsion pendulum measurements. The resulting plots for the stress as a function of the transformed strain rate $a_T R$ at strains

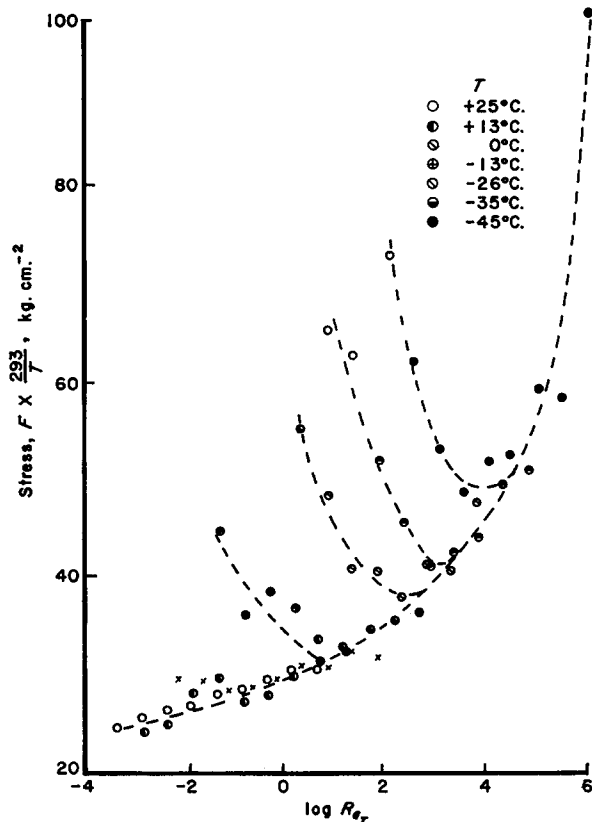


Fig. 5. Master curve of stress vs. strain rate for 400% strain.

of 300 and 400% are shown in Figures 4 and 5; the stresses have been multiplied by the ratio between the chosen reference temperature (293°K.) and the experimental temperature to allow for the temperature dependence of rubberlike elasticity as predicted by the kinetic theory.¹

The graphs show that the transform produces a reasonably well documented master curve at a strain of 280%, but at 440% a set of separate curves is obtained. The stresses at first decrease with increasing rate of elongation, reach a minimum, and then follow the values given by an envelope common to all temperatures. There can be no doubt that this departure from the behavior encountered at lower strains is due to strain-induced crystallization which produces a stiffening of the rubber if the time of elongation is long enough for crystalline regions to form. Taking the actual rate of extension at which the stress curves in Figure 5 have a minimum as a criterion of the least time necessary for appreciable crystallization to occur, the values in Table II are obtained which indicate that crystallization is fastest at -26°C. , in agreement with other findings on the temperature dependence of the rate of crystallization in NR.¹¹ The

TABLE II

Temperature °C.	Time of crystallization, sec.
-13	14.2
-26	4.2
-35	6.8
-45	14.9

envelope in Figure 5 can therefore justifiably be considered as the master curve for the stress in the absence of crystallization.

The contribution of crystallization stiffening to the stress at various strains can be assessed by constructing stress-strain curves from the values given by envelopes such as that in Figure 5 and comparing them with the experimental results. An example is shown in Figure 6 for a rate of extension of 0.5%/sec. at -26°C .

It is obvious from Figure 5 that the stresses cannot be factorized as the product of a strain and a time function over the whole range of experimental variables. Factorization of the stresses is, however, possible for strains below 300% elongation so that, in this range

$$F = f(\epsilon)\varphi(t) \quad (2)$$

where ϵ is the strain and t the time taken to reach this strain at a uniform rate of extension. The experimental evidence will be adduced below in connection with Figure 8. As the function $f(\epsilon)$ approaches ϵ for small strains (Hooke's law), $\varphi(t)$ is seen to be identical with the dynamic Young's modulus. The stress-strain curve for a constant value of t is called isochronal.

In principle, both $f(\epsilon)$ and $\varphi(t)$ can be derived from the experimental data, but the determination of $\varphi(t)$, which governs the dynamic behavior of the rubber, is considerably facilitated if an analytical expression is available for $f(\epsilon)$. Smith⁴ and Landel and Stedry³ have found that the strain

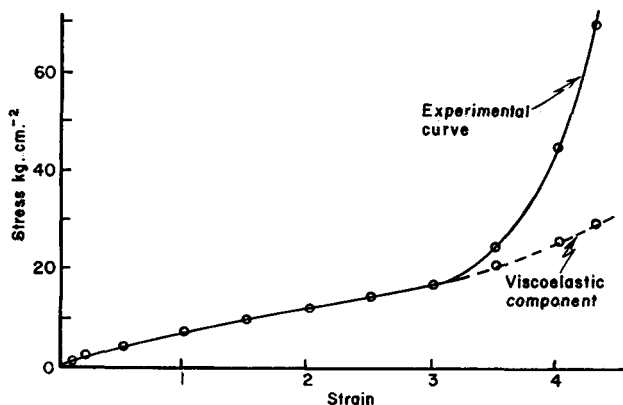


Fig. 6. Resolution of stress into viscoelastic and crystallization components.

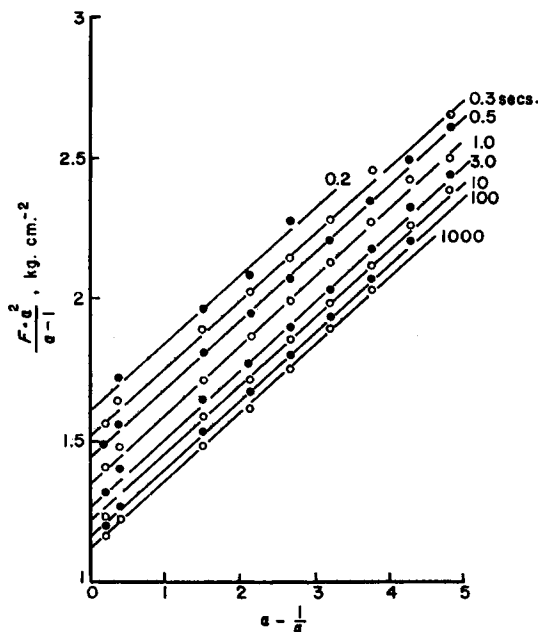


Fig. 7. Isochronal stress-strain data plotted after eq. (3).

function of SBR can be represented by the empirical equation proposed by Martin, Roth, and Stiehler¹² for static stress-strain curves. This equation (MRS equation) is given by eq. (3):

$$F = E[(1/\alpha) - (1/\alpha^2)] \exp \{A[\alpha - (1/\alpha)]\} \quad (3)$$

where α is the extension ratio and A is the slope of the straight line obtained when $\log [\alpha^2 F / (\alpha - 1)]$ is plotted as function of $[\alpha - (1/\alpha)]$. It is easily seen that E is Young's modulus; its logarithm is equal to the intercept of the straight line on the abscissa.

Equating now the factor of E in eq. (3) with $f(\epsilon)$, eq. (2) becomes, after taking logarithms

$$\log [F\alpha^2 / (\alpha - 1)] = \log \varphi(t) + 0.434A[\alpha - (1/\alpha)] \quad (4)$$

The validity of eq. (4) for dynamic stresses is tested by constructing isochronal stress-strain curves for various times $t (= \epsilon/R)$ from the experimental data and plotting, as in the static case, $\log [\alpha^2 F / (\alpha - 1)]$ versus $[\alpha - (1/\alpha)]$. The straight lines in Figure 7, which have been compiled for NR at -45°C ., indicate that eq. (3) is for the present purposes a sufficiently good approximation to the strain function $f(\epsilon)$. As the lines are parallel within the limits of experimental error, with a slope $A = 0.56$, the time function $\varphi(t)$ can be directly derived from the experimentally determined stresses by means of the MRS equation, eq. (3).

Strain-Decreasing Curves

The importance of $\varphi(t)$ lies in the fact that predictions can be made from it as to the stresses during retraction, and hence to the losses.

Equation (2) suggests the applicability of Boltzmann's superposition principle to stresses at large strains, as it has also been surmised by Halpin.¹³ The superposition principle, as originally proposed, is defined only for a linear stress-strain relationship, but eq. (2) can be linearized by writing

$$f(\epsilon) = \epsilon g(\epsilon) \quad (5)$$

where $g(\epsilon)$ is a new strain function. Replacing the strain ϵ by Rt , eq. (2) becomes

$$F/g(\epsilon) = Rt\varphi(t) = R\psi(t) \quad (6)$$

which defines a new time function $\psi(t)$. With the help of eq. (6), the stresses during extension can immediately be used to calculate the stresses during retraction, F_a , by applying the superposition principle, without having recourse to a particular model imitating the viscoelastic behavior of the material. This has been shown by Chang,¹⁴ who derived eq. (7) for a linear system

$$F_a = R\psi(t) - 2R\psi(t - t_m) \quad (7)$$

where t is now the total time elapsed since the stress-strain cycle was started, and t_m is the time at which the maximum strain was reached.

Applying eq. (7) to the linearized stress $F_a/g(\epsilon)$ and taking account of the fact that the strain during retraction is equal to $R(2t_m - t)$, the generalized form of eq. (7) for the stress during retraction is

$$F_a = f(\epsilon)[\psi(t) - 2\psi(t - t_m)]/(2t_m - t) \quad (8)$$

Before proceeding it should be pointed out that the stresses during retraction at various temperatures and rates are not amenable to the Ferry transform because they depend both on t and t_m .

Values of $\psi(t)$ were calculated from stresses during extension to strains up to 300% elongation by using eqs. (5) and (6), with eq. (3) for $f(\epsilon)$. The dependence of $\psi(t)$ on t at -45°C . and $+25^\circ\text{C}$. is shown in the double logarithmic plot in Figure 8. This graph confirms the validity of the factorization, eq. (2), because $\psi(t)$ derived from different stress-strain curves lie on a single curve. This graph contains data obtained with different samples, and small errors in the determination of their cross-sectional area may contribute to the scatter. The scatter is significant only at short elongation times at -45°C .; that is to say, under conditions where sharp maxima occur in the stress-strain curves (Fig. 1) and slight errors in the strain lead to large differences in the value of $\psi(t)$.

The curves for -45°C . and $+25^\circ\text{C}$. merge at long elongation times, and the slope then approaches unity in the logarithmic plot. It is seen from eq. (8) that when $\psi(t)$ is proportional to t , the strain-decreasing stress curve

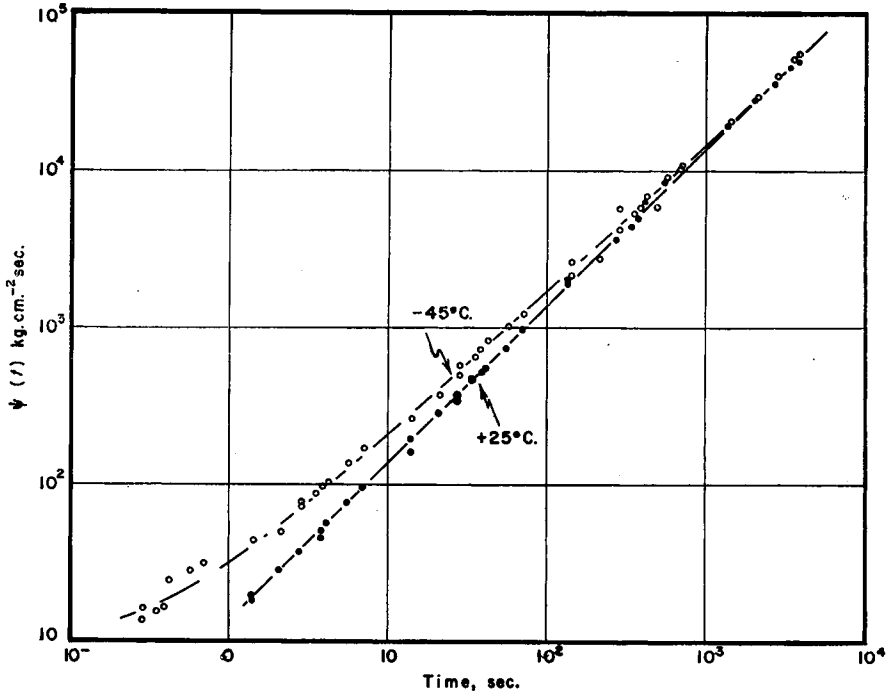
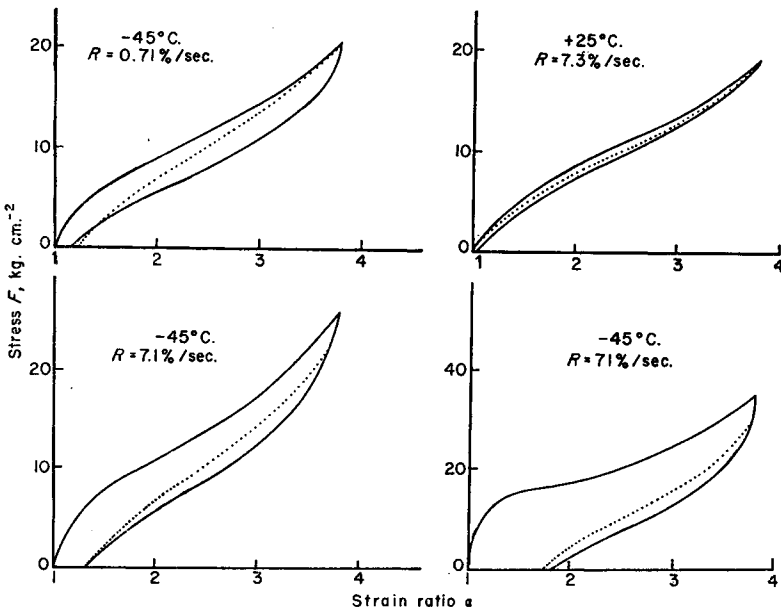
Fig. 8. Plot of $\log \psi(t)$ vs. $\log t$.

Fig. 9. Comparison of (—) experimental and (---) theoretical retraction curves.

coincides with the strain-increasing curve, and the energy losses vanish during slow extension cycles.

Figure 9 shows four experimental stress-strain loops and the corresponding retraction curves calculated from eq. (8). The theoretical retraction curve lies in each case above the experimental one; the difference is very pronounced at low rates of extension, both at $+25^{\circ}\text{C}$. and -45°C ., but becomes progressively smaller with increasing rate of extension. The divergence of the experimental energy losses, i.e., the areas within the loops, from those which would be determined by means of the calculated retraction curves is serious, particularly for slow stress-strain cycles.

The disagreement between theory and experiment cannot wholly be ascribed to crystallization, because the evaluation of data for butadiene-acrylonitrile rubber, given in the earlier publication, produces similar differences between measured and calculated retraction curves. It is thought that the energy losses which thus cannot be accounted for by either viscoelasticity or crystallization are due to stress-softening effects mentioned above. The fact that reproducible stress-strain loops are obtained after several cycles proves only that a stationary state has been reached; reversible stress-softening during subsequent cycles is still feasible.

Two mechanisms have been put forward for stress-softening in gum vulcanizates.⁹ The main contribution is thought to originate from local non-affine deformation due to crosslinks being displaced with respect to their surroundings during extension. This displacement is not easily recovered during retraction. A secondary source of stress-softening is the breakage of labile crosslinks during extension which occurs in vulcanizates of the type used in this work. Both processes are sources of energy loss.

Energy Losses

The rate and temperature dependence of the energy losses incurred during strain cycles with a given maximum elongation should be interrelated by the Ferry transform if they are of viscoelastic origin because only one time factor is involved. An attempt to construct a master curve for the energy loss ratio at a maximum elongation of 280% is shown in Figure 10. In contrast to the stresses attained at this strain during extension (Fig. 4), the energy loss ratio gives separate curves which merge into a common envelope only at high rates of extension. The failure of the energy losses to obey the Ferry transform over the whole experimental range is to be expected from the difference between measured and calculated retraction curves discussed in the last section because both findings demonstrate a departure from a purely viscoelastic loss mechanism. Figure 10 bears a strong resemblance to Figure 5, in which similar divergences of the stress at 440% strain were ascribed to crystallization. It cannot be decided on the present evidence whether the effects shown in Figure 10 are due to crystallization not discernible during extension. It

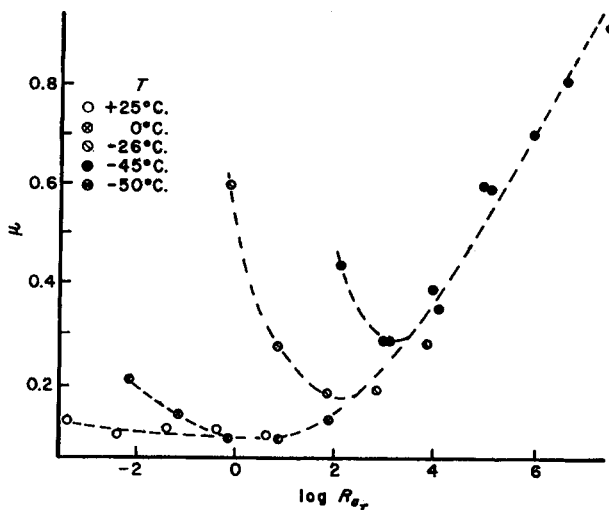


Fig. 10. Master curve of loss ratio μ for 280% strain.

must be borne in mind that the time available for crystallization to develop during the whole strain cycle is longer than during extension alone. Also, recent work by Harwood and Payne suggests crystallization during retraction from strains of about 300%.¹⁵

A survey of the dependence of the energy loss ratio on temperature and strain as function of the elongation time is given in Figure 11. At room temperature (+25°C.), the losses are practically independent of the rate and increase with the maximum strain; the results for -45°C. show one unifying feature in that the loss ratio at elongation times below, say, 4 sec., becomes independent of the strain. As the elongation time increases, the curves have a shallow minimum which occurs the sooner the larger the strain, but it is surprising that the loss ratios at 440% and 530% are practically equal.

This is also true at -26°C.; at this temperature, at which the rate of crystallization is fastest, the loss ratios at the two highest extensions increases slightly with the elongation time. Their approximate constancy is probably fortuitous, viscoelastic losses decreasing and hysteresis due to crystallization increasing, with increasing time. At very short times, the curves for 120 and 280% strain merge again as viscoelastic losses predominate.

Description of the Strain-Increasing Curves

Halpin¹³ has pointed out that if the factorization of the stress according to eq. (2) is possible, the strain function $f(\epsilon)$ must be identical with any expression valid for conditions of thermodynamic equilibrium because the strain function must hold good for very long elongation times. Halpin¹³ showed that stress-strain data obtained from various types of dynamic

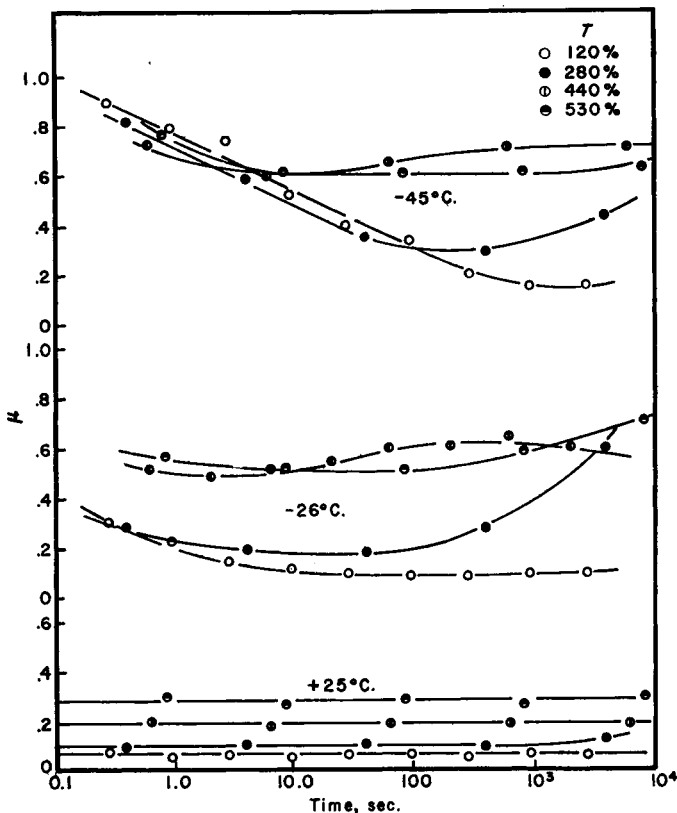


Fig. 11. Energy loss ratio vs. time at different temperatures and strains.

measurements could be fitted to the strain function derived by Treloar¹⁶ from the kinetic theory of rubberlike elasticity. This equation, with a minor approximation introduced by Halpin, is

$$3F/NkT = \sqrt{n}\mathcal{L}^{-1}(\alpha/\sqrt{n}) - 3\alpha^{-2} \quad (9)$$

where N is the number of chain segments between crosslinks and n the statistical number of links in each chain. \mathcal{L}^{-1} stands for the inverse Langevin function. In the dynamic case, NkT in eq. (9) is replaced by $\varphi(t)/3$. The strain function $f(\epsilon)$ is therefore equal to $1/3$ of the right-hand side of eq. (9); this is easily seen by working out eq. (9) for small strains at which it must reduce to

$$F = \varphi(t) \times \epsilon$$

The only adjustable parameter in eq. (9) is n ; for its determination, strain functions were calculated with different values of n , plotted logarithmically and superimposed on the experimental curves to pick out the best fit. The vertical displacement then yields the dynamic modulus $\varphi(t)$. The four examples in Figure 12 show representative results, and

Table III gives the values of $\varphi(t)$ and n used to obtain them; $\varphi(t)$ derived from the MRS equation is listed for comparison.

TABLE III

Temperature, °C.	Extension time, sec.	n	$\varphi(t)$, kg./cm. ²	
			From eq. (9)	From eq. (3)
+25	100	81	12.2	14.4
-35	10	49	12.6	16.9
-45	1	49	17.2	17.0
-50	10	49	36.8	33.0

The values of $\varphi(t)$ determined by the two methods agree reasonably well. It is possibly significant that a larger n had to be used for slow extension at room temperature than for the other conditions. Freedom of rotation around bonds decreases with decreasing temperature and thus reduces the effective number of links in the chains.

Although the theoretical curves in Figure 12 are a fair representation of the experimental results above about 100% strain, serious deviations occur

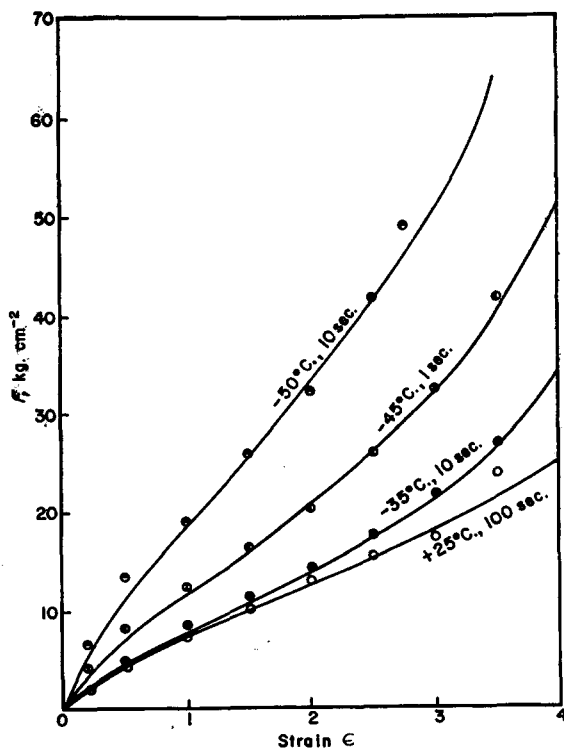


Fig. 12. Isochronal stress-strain curves: (—) calculated from the Treloar-Halpin expression, eq. (9).

at -45°C . and -50°C . at the lower strains. This is where a hump begins to appear in the stress-strain curves (Fig. 1) which is not predicted by the statistical theory. It must furthermore be stressed that both the equation of Martin et al. and Treloar's equation contain only one elastic constant, whereas it is known that the stress at moderate strains, both static and dynamic, is better described by the so-called Mooney-Rivlin equation which contains two constants.⁵ It is interesting to note that these departures from the simple statistical theory disappear at higher strains where it furnishes an adequate strain function and involves only one elastic constant.

Conclusions

The rate and temperature dependence of the stresses developed in natural rubber during extension to high strains conforms, like that of synthetic elastomers, to a viscoelastic pattern if the experimental conditions do not allow appreciable crystallization to occur. The stress can then be factorized as the product of the dynamic Young's modulus and a strain function. This result appears to indicate the validity of the superposition principle, but retraction curves calculated on this basis yield higher stresses and therefore lower losses during a strain cycle than are found experimentally. The agreement between theory and experiment becomes acceptable only at low temperatures and high rates of elongation.

Similarly, the Ferry transform when applied to the mechanical energy losses or to the energy loss ratio, breaks down at rates and temperatures at which the stresses during extension still obey it. There are, thus, mechanisms of energy loss other than viscoelastic which cannot all be attributed to crystallization; stress-softening has been put forward as one possible explanation of this effect.

One unifying feature, and probably the most relevant result obtained in this work, is that the energy loss ratio at short elongation times and low temperatures, where viscoelastic losses predominate, becomes independent of the strain in the experimental range from 120 to 530% elongation.

Part of this work has been submitted by J. A. C. H. as an M.Sc. thesis to the University of Manchester; the work forms part of a research program undertaken by the Natural Rubber Producers' Research Association.

References

1. J. D. Ferry, E. R. Fitzgerald, L. D. Grandine, and M. L. Williams, *Ind. Eng. Chem.*, **44**, 703 (1952).
2. T. L. Smith, *J. Polymer Sci.*, **20**, 89 (1956).
3. R. F. Landel and P. J. Stedry, *J. Appl. Phys.*, **31**, 1885 (1960).
4. T. L. Smith, *Trans. Soc. Rheol.*, **6**, 61 (1962).
5. A. Schallamach, D. B. Sellen, and H. W. Greensmith, *Brit. J. Appl. Phys.*, **16**, 241 (1965).
6. K. A. Grosch and A. Schallamach, *Inst. Rubber Ind. Trans.*, **41**, 80 (1965).
7. L. Mullins and N. Tobin, *Proc. 3rd Rubber Technol. Conf. (London, 1954)*, p. 397 (1956).

8. J. A. C. Harwood, L. Mullins, and A. R. Payne, *J. Appl. Polymer Sci.*, **9**, 3011 (1965).
9. J. A. C. Harwood and A. R. Payne, *J. Appl. Polymer Sci.*, **10**, 1203 (1966).
10. M. L. Williams, R. F. Landel, and J. D. Ferry, *J. Am. Chem. Soc.*, **77**, 3701 (1955).
11. A. N. Gent, *J. Polymer Sci.*, **18**, 321 (1955).
12. G. M. Martin, F. L. Roth, and R. D. Stiehler, *Inst. Rubber Ind. Trans.*, **32**, 189 (1956).
13. J. C. Halpin, *J. Polymer Sci. B*, **2**, 959 (1964).
14. F. S. C. Chang, *J. Appl. Polymer Sci.*, **8**, 37 (1964).
15. J. A. C. Harwood and A. R. Payne, *J. Appl. Polymer Sci.*, in press.
16. L. R. G. Treloar, *Trans. Faraday Soc.*, **50**, 881 (1954).

Résumé

Les étirements et les pertes d'énergie au cours de cycles d'extension simples jusqu'à un maximum de 530% ont été déterminés pour un vulcanisat chargé de caoutchouc naturel en fonction de la température et de la vitesse d'extension. A des temps d'élongation suffisamment courts et des températures basses, la dépendance de la vitesse et de la température des extensions croissantes sont reliées par l'équation de Ferry et le principe de superposition peut leur être appliqué. Outre ce domaine expérimental, les étirements sont accrus par cristallisation. La validité de l'équation de Ferry pour les pertes d'énergie et le rapport de perte d'énergie est plus fortement limitée que pour les étirements et les pertes sont toujours plus élevées que celles prévues au départ d'un mécanisme purement viscoélastique. Des pertes additionnelles sont attribuées à titre d'essai à une cristallisation débutante et à des effets de ramollissement par étirement. A des temps d'élongation courts à basse température, les pertes s'approchent des valeurs prévues par la viscoélasticité et le rapport de perte devient indépendant de l'extension maximum du cycle de tension.

Zusammenfassung

Spannungen und Energieverluste während einfacher Dehnungszyklen bis zu einer maximalen Elongation von 530% wurden an einem ungefüllten Naturkautschukvulkanisat als Funktion der Temperatur und Dehnungsgeschwindigkeit bestimmt. Bei genügend kurzen Dehnungsdauern und niedrigen Temperaturen werden Geschwindigkeits- und Temperaturabhängigkeit der ansteigenden Spannungen durch die Ferry-Transformation verknüpft und das Superpositionsprinzip kann darauf angewendet werden. Ausserhalb dieses experimentellen Bereiches werden die Spannungen durch Kristallisation vergrössert. Die Gültigkeit der Ferry-Transformation für die Energieverluste und das Energieverlustverhältnis ist stärker eingeschränkt als für die Spannungen und die Verluste sind immer höher als für einen rein viskoelastischen Mechanismus erwartet werden kann. Die zusätzlichen Verluste werden versuchsweise einer beginnenden Kristallisation und Spannungserweichungseffekten zugeschrieben. Bei kurzen Dehnungsdauern und niedrigeren Temperaturen nähern sich die Verluste den durch die Viskoelastizität bedingten Werten und das Verlustverhältnis wird von der maximalen Dehnung während des Verformungszyklus unabhängig.

Received January 30, 1967
Prod. No. 1576